Algal Research 64 (2022) 102685

Contents lists available at ScienceDirect

Algal Research

journal homepage: www.elsevier.com/locate/algal

Effects of LED lighting on *Nannochloropsis oceanica* grown in outdoor raceway ponds

M. Carneiro [a], I.B. Maia [b], P. Cunha [c], I. Guerra [c], T. Magina [d], T. Santos [b], P.S.C. Schulze [e], H. Pereira [e], F.X. Malcata [a], J. Navalho [d,e], J. Silva [c,e], A. Otero [f], J. Varela [b,e,*]

[a] *LEPABE – Laboratory for Process Engineering, Environment, Biotechnology and Energy, Faculty of Engineering of the University of Porto, Rua Dr. Roberto Frias, 4200-465 Porto, Portugal*
[b] *CCMAR – Centre of Marine Sciences, University of Algarve, Gambelas, 8005-139 Faro, Portugal*
[c] *Allmicroalgae Natural Products S.A., R&D Department, Rua 25 de Abril 19, 2445-287 Pataias, Portugal*
[d] *Necton S.A., Belamandil, 8700-152 Olhão, Algarve, Portugal*
[e] *GreenCoLab - Associação Oceano Verde, University of Algarve, Campus de Gambelas, Faro, Portugal*
[f] *Instituto de Acuicultura and Departamento de Microbiología y Parasitología, Facultad de Biología, Universidade de Santiago de Compostela, 15782 Santiago de Compostela, Spain*

A R T I C L E I N F O

Keywords:
Artificial light
Nannochloropsis
Productivity
Raceway pond
Circadian cycle

A B S T R A C T

Growth in most microalgal mass cultivation systems is light-limited, particularly in raceway ponds (RWP) where the light path is higher. Artificial lighting can be a promising solution to diminishing dark zones and enhance microalgal productivity. Therefore, our goal was to prevent the cell shift from photosynthesis to a respiration-only stage by resorting to LED illumination. *Nannochloropsis oceanica* cultures were accordingly grown outdoors in a preliminary small-scaleexperiment, followed by pilot-scale trials. In the former, three 3.0-m^2 RWP were set up under three distinct conditions: 1) without LEDs (control); 2) LEDs turned on during the night; and 3) LEDs turned on for 24 h. In the pilot-scale trial, one of two 28.9-m^2 pilot-scale RWPs was coupled to the best LED setup – determined in the small-scale preliminary experiment – using the same light intensity (normal mode) and half of the intensity (economy mode), with the second RWP serving as a control. In the preliminary experiment, the use of LEDs for 24 h was deemed as not helpful during daytime, before the culture reached ≈0.5 g DW L^{-1} – when dark zones appeared during the day due to sunlight attenuation in the 0.1 m-deep cultures. Overall, use of LEDs increased biomass growth chiefly by increasing nighttime productivities – materialized in higher chlorophyll, protein, and carbohydrate productivities in LED-lit cultures. A higher impact of LED lighting was observed under lower sunlight irradiances. A preliminary economic analysis indicates that use of LEDs in RWPs outdoors should be considered for high-value metabolites only.

1. Introduction

Currently, the expanding range of microalgae applications in various commercial sectors drives the growing demand for microalgal biomass and its derivatives. In turn, this pushes microalgae production facilities to improve their supply by increasing production as well as enhancing the process efficiency. However, any putative strategy towards this end must be carefully assessed, otherwise production costs may go beyond the biomass selling price. Industrial production systems for microalgal cultivation comprise closed or open systems, which differ significantly in productivity and costs. The former require substantial investment [1], but productivities can reach 10 to 45 g m^{-2} day^{-1} [2–4]. On the other hand, open production systems, such as raceway ponds (RWP), are considered to be one of the cheapest microalgae production systems [5] – even though at the expense of lower productivities, typically from 12 to 28 g m^{-2} day^{-1} [4–6]. Further disadvantages include higher susceptibility to contamination by other microalgae, predators (e.g., rotifers and amoebae), and parasites (e.g., cryptofungi and chytrids), low CO_2 absorption, high O_2 build-up, and poor light distribution within the culture. Additionally, outdoor microalgae production systems are exposed to the elements (e.g., high variances in irradiance, temperature, humidity) with daily and seasonal fluctuations resulting in increased difficulties to control temperature, avoid photo-limitation and photo-inhibition, among others. From all these factors, light has always been

* Corresponding author.
E-mail address: jvarela@ualg.pt (J. Varela).

https://doi.org/10.1016/j.algal.2022.102685
Received 31 May 2021; Received in revised form 15 October 2021; Accepted 19 March 2022
Available online 29 March 2022

one of the major growths controlling factors in microalgae cultivation, particularly in RWP. This is due to the fact that RWP present one of the largest light paths – commonly found between 10 and 30 cm [7–12] – compared to other commercial systems such as tubular photobioreactors with 2.5–14 cm [13,14], and flat panel photobioreactors (FP-PBR) with 4.5–9 cm [15,16]. Moreover, RWPs are limited to a one directional light exposure as opposed to the other mentioned cultivation systems. This makes light one of the most limiting factors in RWP-cultivation. Light penetration in algal cultures is also severely limited beyond 5 cm depth in algal concentrations above 0.3 g L^{-1}, meaning beyond this depth is virtual darkness where no photosynthetic processes occur [7]. One solution that was put forward was the use of thin-layer systems with a column depth of ca. 0.5–5.0 cm, shading in these systems is quite low, but in the summer can also lead to lower photosynthetic efficiencies [17]. Therefore, the search for improvements in cultivation systems is still an ongoing process.

The utilization of artificial light has been extensively studied and can boost productivity, provide more stable and controllable growth conditions, and induce synthesis of specific metabolites [18–22]. Although most industrial facilities producing autotrophic microalgae rely on natural lighting, artificial light has been routinely employed indoors at some facilities. Although LEDs have proven to be more efficient than other artificial light sources [23] they can still have a severe impact on production costs. Therefore, for mass cultures, the use of LEDs for artificial lighting must be coupled to the production of high-value products (e.g., omega-3 polyunsaturated fatty acids (PUFA) and astaxanthin) to balance the economic feasibility of the whole bioprocess. Several studies have focused on microalgae cultivation in RWP indoors using artificial lighting [11,24], such as the previous study by Hueseman et al. (2017) that tested the ability of 800-L LED-lit indoor RWPs to simulate microalgae growth outdoors [8]. However, to our knowledge, no studies focused on the use of LEDs to increase productivity in RWPs outdoors are available – probably due to the clash between a low-cost cultivation system (RWP) and a high-cost upgrade (LEDs). Nonetheless, the integration of artificial lighting to improve biomass productivity merits to be explored, in attempts to ascertain the accompanying efficiency under outdoor conditions.

The current work consequently assessed the use of LEDs under outdoor conditions, with *Nannochloropsis oceanica* as model culture. This work focused on both the use of LED lighting during the night, when biomass losses usually occur, and for 24 h, since sunlight penetration can be impaired by high biomass concentration, large depth of the water column or low irradiance. Therefore, a preliminary experiment in small-scale 3.0-m^2 RWPs was carried out to evaluate the use of LED lighting during the night and for 24 h. Afterward, the best setup was tested at pilot-scale, using 28.9-m^2 RWPs under two different light configurations. To ascertain the increase in biomass cost due to LED lighting, a simple economic analysis was performed – which helped to assess the economic feasibility of implementing LED systems in low cost RWPs.

2. Material and methods

Two trials were performed. The small-scale preliminary experiment took place at Necton S.A. facilities (Olhão, Portugal), between January 21st and May 8th, 2019. The subsequent pilot-scale trial was carried out at Allmicroalgae S.A. facilities (Pataias, Portugal), between March 17th and July 13th, 2020.

2.1. Microorganisms, media, and inocula

Commercial strains of the *Nannochloropsis* genus were used in each facility and trial – *Nannochloropsis* oceanica NAS0197 in Necton S.A. for the small-scale preliminary experiment, and *Nannochloropsis oceanica* CCAP 849/10 in Allmicroalgae S.A. for the pilot-scale trial. Both strains were pre-cultured in the laboratories in aerated (1% CO_2) round bottom 5-L flasks and subsequently used to sequentially inoculate three FP-PBR of 100, 400, and 800 L outdoors – consisting of a plastic bag with 0.08 m width supported by a metal structure with filtered aeration and a CO_2 injection pulse system. The FP-PBR was, in turn, used to inoculate a pilot-scale tubular photobioreactor (PBR) with CO_2 injection on demand, with volumes of 3.2 and 2.5 m^3 for the small-scale preliminary experiment and pilot-scale trials, respectively. The resulting cultures served as inoculum in the experiments implemented afterward.

Cultures were grown in natural and artificial seawater (in the small-scale preliminary experiment and pilot-scale trials, respectively), adjusted to a salinity of 33 g L^{-1}. Seawater was supplemented with a concentrated culture medium based on Guillard's f/2 [25]: NutriBloom® Plus medium (Phytobloom by Necton, Portugal) [26] for the small-scale preliminary experiment and Allmicroalgae's base medium (f/2 medium [25]) for the pilot-scale trial. Nitrate concentration was monitored as per the NO_3 ultraviolet spectrophotometric standard method [27]. Whenever nitrate levels reached 5 mM, complete medium was added up to a concentration of 8–9 mM NO_3 to ensure sufficient nutrient availability.

2.2. Experimental setup

2.2.1. Small-scale preliminary experiment

Three identical 300-L RWPs, with a surface area of 3.0 m^2, were used to cultivate the microalgae outdoors at Necton's facilities (Olhão, Portugal). The RWPs consisted of two channels (0.39 m wide each) and a deflector baffle at each bend. The length of the channel's straight zones measured 3.21 m; in one of the channels, the paddle wheel was placed 1.76 m from the bend. The RWPs were equipped with dissolved O_2 and temperature probe (SUP-DM2800, Supmea, China), and pH probe (SUP-PH5013A, Supmea, China), all connected to a Supervisory Control and Data Acquisition (SCADA) control system. This system was also connected to a WatchDog WD-2700 meteorological station, coupled to a LICOR LI-190R-BL-15 quantum sensor installed at the facility and able to provide real-time weather data. The pH was pre-set at 8.1, with automatic addition of CO_2 when needed.

Since lighting RWP cultures from above would diminish sunlight penetration, and most RWPs are either opaque or buried in the ground, submersible LEDs were employed. Four LED strips (Fig. 1A) of 3.2 m, and four of 1.75 m of length were evenly separated, strapped to two rigid inox structures of compatible length (which helped to remove the LEDs for more intensive cleaning of the RWP), and placed at the bottom of the RWP (Fig. 1B). The 0.07 m-interspace between LEDs was defined to minimize "overlapping" irradiance between LED strips and maximize homogenous light distribution from the bottom of the RWP (Fig. 1C). The LED strips covered 65% of the RWP's total area and provided an estimated maximum power density of 72 W m^{-2}.

Each 3.0-m^2 RWP was operated as one of three independent conditions: a RWP without LEDs (control), a RWP where the LEDs were turned on only during the dark periods (night LED), and the third RWP with LEDs turned on permanently for 24 h (24 h LED). The three different conditions were run simultaneously, starting from a culture concentration of ca. 0.12 g of biomass dry weight (DW) L^{-1} and a culture depth of 0.10 m. Cultures were grown batchwise for 9 days, and the experiment was repeated three times. The first, second, and third runs were performed from January 21st to the 30th, from April 5th to the 14th, and from April 30th to May 8th of 2019, respectively.

Biomass sampling was done twice a day, in the morning (08:30) and evening (17:00). Birch plywood covers were built and used to cover the cultures (Fig. 1D) to control the light:dark cycles (8.5L:15.5D). Cultures were covered after the evening sample was taken (sampling occurred in the light) and were left uncovered after the morning sample (sampling occurred in the dark).

2.2.2. Pilot-scale trial

A larger pilot-scale trial was performed at Allmicroalgae's facilities (Pataias, Portugal), using two outdoor 3754-L RWPs with a surface area of 28.9 m^2. The straight channels measured 13.2 m in length, and the

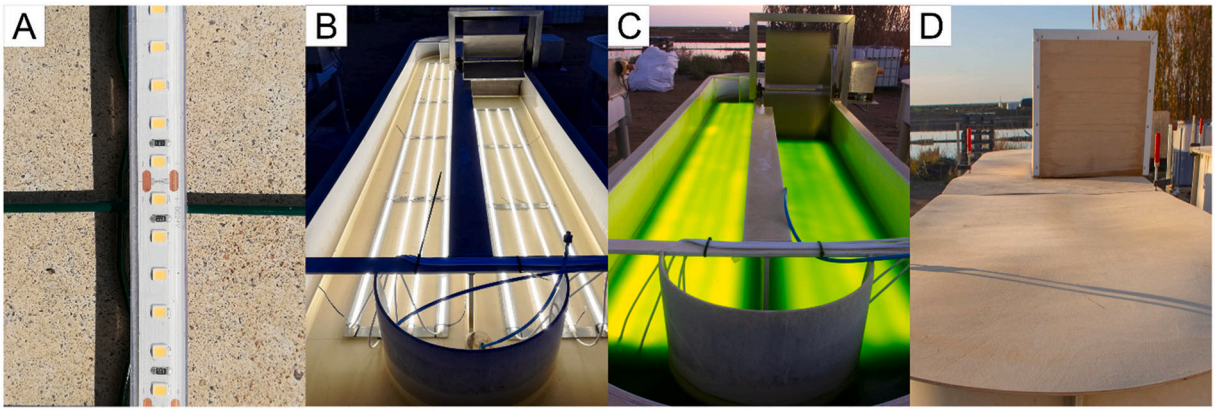

Fig. 1. LED installation in the 3.0-m^2 RWPs for the small-scale preliminary experiment. Close-up of the LEDs used in this study (A); water-submerged LEDs at the bottom of the RWP during the night (B); RWP illuminated with LEDs in the evening and submerged in a *Nannochloropsis oceanica* culture (C); and birch plywood covers used to control the diel cycle (D).

paddlewheel was located just after the bend [28].

In these pilot-scale trials, one RWP corresponded to the control, while the second RWP received supplementary irradiance with LEDs. Culture growth in the LED-lit RWP comprised two stages. In the first one, LEDs were turned on only during the night (night LED), until the culture reached a predetermined concentration (ca. 0.5 g DW L^{-1} defined by the small-scale preliminary experiment). The second stage was initiated afterward, and the LEDs were left on for 24 h (24 h LED) until the end of the experiment. Cultures from both control and LED-lit 28.9-m^2 RWPs were carried out simultaneously, starting from a culture concentration of ca. 0.30 g DW L^{-1} and a culture depth of 0.13 m (minimum water depth for adequate mixing in these RWPs). Sampling was done twice a day, in the morning (08:00) and evening (18:00).

This pilot-scale trial was composed of two independent sub-trials, comprising two different LED setups (LED quantity and light intensity): the normal and economy modes described below.

2.2.2.1. Normal mode. In the normal mode, LED power density was adjusted to 72 W m^{-2} to mimic the one used in the small-scale preliminary experiment. Ten rows of LED strips of 12.0 m and ten of 11.0 m in length were strapped, 0.08 m apart, to two plasticized electro-welded meshes and then placed at the bottom of the 28.9-m^2 RWP (Fig. 2A and B), thus covering 76% of the RWP area. Cultures were grown in batch mode for 10 days until culture concentrations reached 1 g DW L^{-1}. The experiment was repeated another two times. The first, second, and third runs were performed from the June 4th to the 15th, from June 22nd to July 2nd, and from July 3rd to the 13th of 2020, respectively.

2.2.2.2. Economy mode. In the economy mode experiment, the number of LEDs was decreased to provide a power density of 29 W m^{-2}. Four LED strips of 12.0 m and four of 11.0 m were mounted 0.19 m apart to homogenize light distribution throughout the 28.9-m^2 RWP channels and covering 76% of the RWP total area (Fig. 2C and D). Cultures were grown in batch mode for 15 days, and the experiment was performed three times. The first, second, and third runs were performed from March 17th to April 1st, from April 2nd to the 17th, and from April 17th to May 2nd, of 2020, respectively.

2.3. LED

Warm white (2700 K) IP68 LED (2835, 24 V, 1280 Lm m^{-1}, 14.4 W m^{-1}, JustLIGHT, China) strips, with a luminous efficacy of 88.9 lm W^{-1}, were used in all trials (the corresponding emission spectrum is provided in Supplementary Fig. S1). The LEDs were operated in parallel, using a constant voltage power supply (24 V DC, 12.5 A, 300 W, IP66). The energy, expressed in mole of photons (E), was determined based on Planck's equation as per Eq. (1):

$$E\left(\text{J µmol of photons}^{-1}\right) = \frac{h \times c \times N_A}{\lambda \times 10^6} \quad (1)$$

where h is Planck's constant (6.626×10^{-34} J s^{-1}), c is the speed of light (299,792,458 m s^{-1}), N_A is Avogadro's number (6.022×10^{23} mol^{-1}) and λ is the dominant wavelength of the LED used (6.07×10^{-11} m). The maximum intensity of radiant energy was then calculated by considering the total power provided and assuming an energy to power conversion efficiency of 50% [29], see Eq. (2) for W m^{-2} and Eq. (3) for µmol m^{-2} s^{-1}:

$$P_{\text{opt } max}\left(\text{W m}^{-2}\right) = \frac{L \times \Phi_{e,\lambda} \times 0.5}{A_i} \quad (2)$$

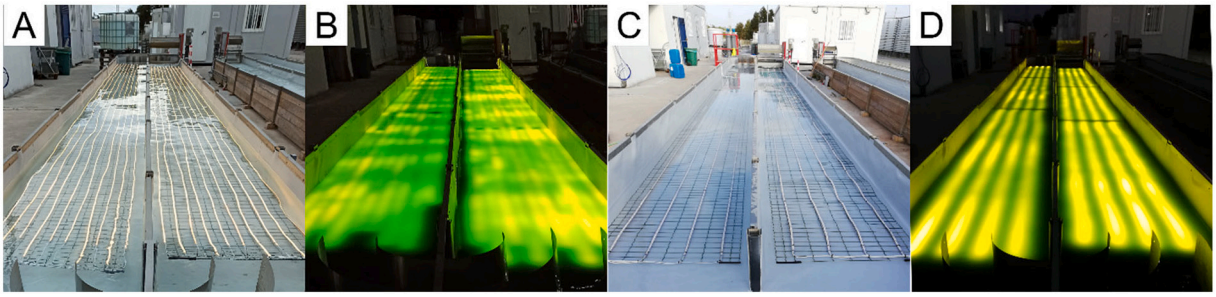

Fig. 2. LED installation in the 28.9-m^2 RWP used in the pilot-scale trials. Panels A and B show the submerged LEDs used for the normal mode without (A) and with (B) *N. oceanica* culture in the afternoon and at night, respectively. Panels C and D show the LEDs setup for the economy mode without (C) and with (D) culture in the morning and at night, respectively.

$$I_{max}\ (\mu mol\ m^{-2}\ s^{-1}) = \frac{L \times \Phi_{e,\lambda} \times 0.5}{A_i \times E} \quad (3)$$

where L pertains to the total LED length used, $\Phi_{e,\lambda}$ to the LED's spectral flux (14.4 W m^{-1}), and A_i to the LED illuminated area of the RWPs.

2.4. Measurements

2.4.1. Growth

Growth was assessed using a calibration curve between biomass DW and optical density (OD). Measurements of DW were performed in duplicate, by filtering 10 mL of culture through pre-weighed 0.7 μm-glass microfiber filter membranes (698, VWR). The biomass on the filters was washed with 10 mL of ammonium formate (35 g L^{-1}), and oven-dried at 60 °C until constant weight [3,30]. The OD of the same samples was measured using a spectrophotometer (UVmini-1240, Kyoto, Japan in the small-scale preliminary experiment, and Genesys 10S UV-VIS, Thermo Fisher Scientific, in the pilot-scale trials), both at 540 nm.

Specific areal productivities (P_s), between measurements during the day and night periods, were determined according to Eqs. (4) and (5), respectively:

$$\text{Daytime } P_s\ (g\ m^{-2}d^{-1}) = \frac{X_{evening(n)} - X_{morning\ (n)}}{(t_{evening(n)} - t_{morning\ (n)}) \times A} \quad (4)$$

$$\text{Nighttime } P_s\ (g\ m^{-2}d^{-1}) = \frac{X_{morning\ (n+1)} - X_{evening\ (n)}}{(t_{morning\ (n+1)} - t_{evening\ (n)}) \times A} \quad (5)$$

where $X_{evening\ (n)}$ and $X_{morning\ (n)}$ correspond to the biomass (g) of the culture on the same day "n" in the evening and morning, respectively, and $X_{morning\ (n+1)}$ to the biomass on the morning of the following day, whereas A (m^2) corresponds to the RWP's surface area occupied by the culture.

2.4.2. Fluorescence measurements

Off situ chlorophyll *a* fluorescence measurements were carried out in the small-scale preliminary experiment, using the pulse-amplitude-modulated fluorimeter AquaPen (AP 110-C, Photon Systems Instruments, Czech Republic), coupled with FluorPen (version 1.0) software. Samples were pre-diluted to an OD_{540} of ca. 0.6 and incubated for 15 min in the dark to oxidize all plastoquinone (Q_A). Individual samples were used for the manufacturer protocol of rapid-light curves (RLC; protocol LC3). The light intensity to induce minimal chlorophyll fluorescence (measuring light) was set to 0.014 μmol photon m^{-2} s^{-1}, whereas the saturating light to induce maximal chlorophyll fluorescence was set at 2400 μmol photon m^{-2} s^{-1}. Using the results from the default LC3 protocol, the relative electron transport rate (rETR) was determined based on Genty's relationship [31], as conveyed by Eq. (6):

$$rETR = \frac{\Delta F}{F'_m} \times I_i \quad (6)$$

where I_i is the incident photosynthetic photon flux density (μmol photon m^{-2} s^{-1}), thus leaving rETR to be expressed in μmol photon m^{-2} s^{-1}. Rapid light curves were fitted by the Eilers and Peeter's model (1988) [32]. The corresponding light-saturation parameter (E_k) was determined according to Eq. (7):

$$E_k = \frac{rETR_{max}}{\alpha} \quad (7)$$

where α represents the initial slope of the rETR curve and $rETR_{max}$ the highest value of rETR.

2.4.3. Pigments

Pigment extraction was performed on fresh biomass as described in Carneiro et al. (2020), using chlorophyll *a* and carotenoid equations based on SCOR-UNESCO (1966) and Jaspars (1965), respectively [33–35].

2.4.4. Gross biochemical composition

Culture samples were centrifuged and pooled to remove most of the water, and the remaining pellet was lyophilized (LyoQuest Telstar, Terrassa, Spain). The resulting dried biomass was stored at −20 °C until use for subsequent analysis.

2.4.4.1. Lipid content. According to Bligh and Dyer (1959), lipid content was determined by gravimetry with slight modifications in the disruption method, since an IKA Ultra-Turrax disperser (IKA-Werke GmbH, Staufen, Germany) was used [36,37].

2.4.4.2. Protein content. Protein content was determined by elemental analysis of total nitrogen as per manufacturer's procedure, using a Vario EL III (Elementar Analysensysteme GmbH, Germany). Total nitrogen content was later multiplied by the conversion factor 4.95 to obtain the total protein content [38].

2.4.4.3. Ash content. Approximately 50 mg of biomass were incinerated in a furnace (J.P. Selecta, Sel horn R9-L coupled with a program controller TC88, Bentrup) for 8 h at 525 °C. Differences in weight between pre- and pos-incinerated biomass were calculated.

2.4.4.4. Carbohydrate content. Total carbohydrate content was determined by difference, by subtracting lipid, protein, and ash results from 100%.

2.4.5. Fatty acid analysis

Extraction and conversion of samples to fatty acid methyl esters (FAME) were done following a protocol by Folch et al. (1957) and Lepage and Roy (1984), with modifications described by Pereira et al. (2012) [40,41]. Briefly, lyophilized biomass samples were resuspended in a methanol:acetyl chloride solution (20:1 v/v) and homogenized with an Ultra-Turrax disperser (1.5 min at 23000 rpm; T18 digital ULTRA-TURRAX, IKA-Werke GmbH & Co. KG, Staufen, Germany). Derivatization took place, after adding *n*-hexane, at 70 °C for 1 h. The lipidic phase was separated by vortexing the samples with distilled water and hexane, followed by centrifugation (this step was repeated thrice). Residual water was removed with anhydrous sodium sulfate. Extracts were filtered, dried under a nitrogen gas flow, and resuspended in GC grade hexane. The analysis was performed in a Bruker gas chromatograph, coupled with a mass spectrometry (MS) detector (Bruker SCION 456/GC, SCION TQ MS) equipped with a ZB-5MS capillary column (30 m × 0.25 mm internal diameter, 0.25 μm film thickness, Phenomenex), using helium as the carrier gas. The GC oven temperature profile was set to 60 °C (1 min), 30 °C min^{-1} to 120 °C, 5 °C min^{-1} to 250 °C, and 20 °C min^{-1} to 300 °C (2 min). Calibration curves were prepared with the commercial standard Supelco® 37 Component FAME Mix (Sigma-Aldrich, Sintra, Portugal). Results are expressed as percent of total fatty acid content.

2.5. Economic analysis

The economic analysis for the LEDs used in the pilot-scale trials includes only the higher capital investments (LED strips and power supplies; $CAPEX_{LED}$) and operational costs (electricity; $OPEX_{LED}$) – determined according to the local cost of electricity and an operation of 330 days per year. A conservative average usable life of 30.000 h for the LEDs and the power supply were considered for capital depreciation. Means of the resulting biomass in each mode were used as a proxy for the biomass produced – without including seasonal variations. The values presented of additional biomass produced are relative to the corresponding control (without LEDs). Hence, a detailed evaluation of CAPEX and OPEX expenses pertaining to the control was not included, since

they do not significantly affect comparison between LED treatments – besides falling outside the scope of this work.

2.6. Statistical analysis

The three runs of each trial were aimed at determining the average with the respective standard deviations. Using these averages, an ANOVA followed by a posthoc – Tukey's test – were used to determine significant differences between conditions (control, LED night, and 24 h LED), at a significance level of $\alpha = 0.05$. When data were of a non-parametric nature, a Kruskal-Wallis test was used. A paired *t*-test was used to compare evening and morning samples of the same condition. All statistical analyses and resulting plots were performed using R software.

3. Results & discussion

3.1. Small-scale preliminary experiment

3.1.1. Growth

The implementation of LEDs in RWPs outdoors was first evaluated in small scale 3.0-m^2 RWPs. Starting at a concentration of 0.12 ± 0.01 g DW L^{-1}, the cultures grew for 9 days in batch, and the growth of individual runs, and the average of the three repetitions are shown in Fig. 3. Meteorological data, including irradiance and temperature for each run of this experiment, are provided in Supplementary Figs. S2 and S3, respectively.

By the end of the trial, the cultures reached on average 1.00 ± 0.18, 1.52 ± 0.49, and 1.8 ± 0.68 g DW L^{-1} for the control, night LED, and 24 h LED cultures, respectively. The beneficial effect of using LEDs is perceptible just after 24 h and increased over time. Beyond the 4th day, the night LED and 24 h LED cultures reached a ratio to the control of 1.38 ± 0.12 and 1.64 ± 0.13, respectively. Important differences in growth can be observed between the first run, performed in late January, and the third run, performed in early May, which caused higher standard deviations in the averaged values (Fig. 3). This difference can be explained by the meteorological conditions, especially sunlight irradiance, which differed substantially between runs (see Supplementary Fig. S2). Nevertheless, a significant beneficial effect of LED illumination ($p < 0.05$) was found, using the average values of the three runs.

A crucial point in these growth curves is when the night LED culture and the 24 h LED culture started to diverge, with the 24 h LED culture growing faster during the day. This effect becomes visible in the averaged values in Fig. 3D after day 3, when the night LED culture reached 0.57 g DW L^{-1}. From this point forward, sunlight could no longer penetrate down to the bottom of the 3.0-m^2 RWPs, as determined with a lux meter placed below an analogous replica of the RWP channel, with a transparent bottom filled with biomass at the same concentration as the RWP (data not shown). This can also be seen in Supplementary Table S1, which shows the areal productivities for each growth phase: lag, logarithmic and late logarithmic, where LED-lit culture do not show any differences, and which only appear in the logarithmic phase. This light attenuation with column depth and biomass concentration proves one of the major constraints when using RWPs for microalgae cultivation [42], and explains the observed improvement when LEDs were applied.

To clarify the LED's impact on the culture's growth during the day and nighttime that were masked by the differences between runs (see Fig. 3), specific areal productivities of each run (boxplots) and their average (violin plot) are detailed in Fig. 4.

The higher data dispersion in the average daytime productivities (violin plots of Fig. 4) was chiefly due to the higher weather variability conditions during the day particularly light and temperature, as during the night irradiance was steadily provided only by the LEDs. Hence, differences in night productivities among conditions became more apparent, with a significantly ($p < 0.05$) lower mean areal productivity for the control (2.3 ± 5.0 g m^{-2} d^{-1}) compared to those of the night LED (9.1 ± 7.2 g m^{-2} d^{-1}) and 24 h LED (11.6 ± 8.5 g m^{-2} d^{-1}) cultures

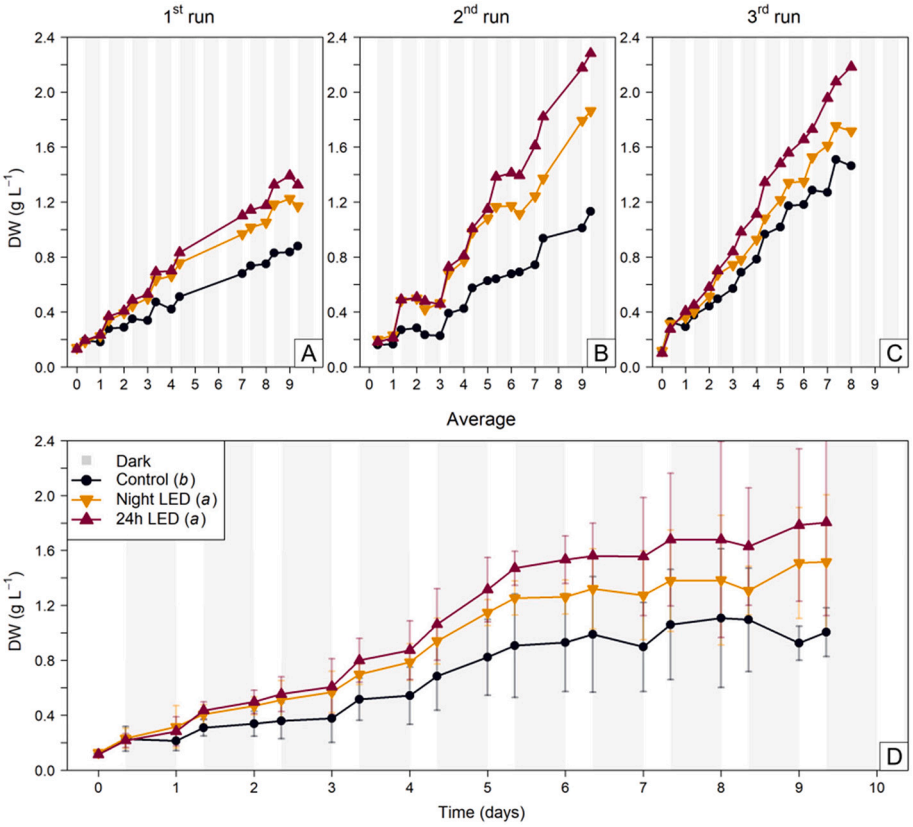

Fig. 3. Growth, in terms of g of dry weight (DW) L^{-1}, over time (days) of *Nannochloropsis oceanica* grown in batch under three different conditions: without LEDs (control; dark grey circles), with LEDs turned on during the night (Night LED; yellow inverted triangles) and with LEDs turned on for 24 h (24 h LED; red triangles) in three 3.0-m^2 raceway ponds (RWP) outdoors. The RWPs were manually covered between evening and morning samples, to control the dark periods and simulate nighttime (light grey vertical bars). Data from each run performed in January (A), April (B), and Late May (C), and the averaged values of the three (D) are shown. Conditions that do not share a letter (in brackets in the inset legend in the average plot) represent significant differences ($p < 0.05$). Error bars represent standard deviations. (For interpretation of the references to colour in this figure legend, the reader is referred to the web version of this article.)

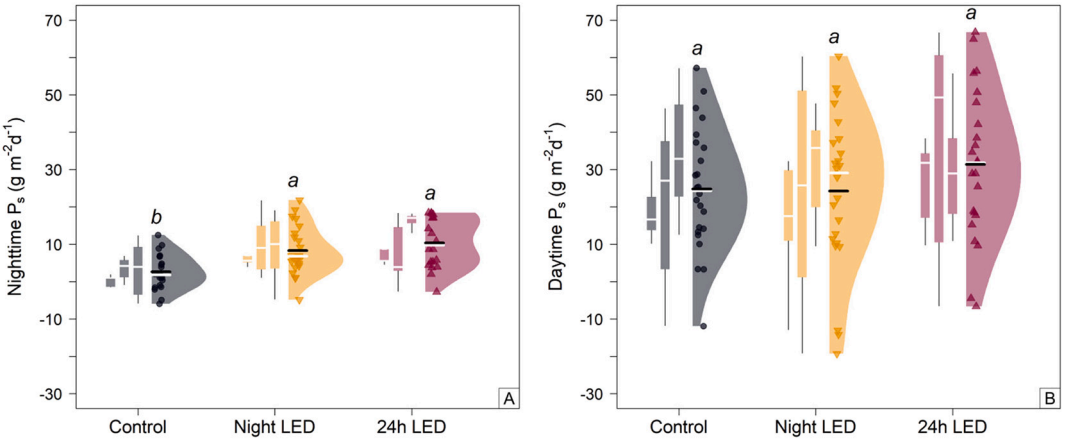

Fig. 4. Comparison of specific areal productivities (g m^{-2} d^{-1}) during the night (Nighttime P_s; A) and day (Daytime P_s; B) periods of *Nannochloropsis oceanica* cultures grown in outdoor 3.0-m^2 raceways ponds without LEDs (Control; dark grey), with LEDs turned on during the night (Night LED; yellow) and with LEDs turned on for 24 h (24 h LED; red). The three boxplots represent the values for the first, second, and third runs, in this order. The violin plot combines the values of all three runs. The values that compose the violin plot are depicted as dots inside the violin region (Daytime P_s: $n = 24$; Nighttime P_s: $n = 21$). Horizontal white lines for both boxplots and violin plots represent the median, while the horizontal black line in the violin plot represents the average. Conditions that do not share a letter (on top of each violin plot) represent significant differences ($p < 0.05$). (For interpretation of the references to colour in this figure legend, the reader is referred to the web version of this article.)

(Fig. 4A). However, average daytime productivities (Fig. 4B) did not vary significantly between conditions and exhibited a wider dispersion of values than their nighttime counterparts – reaching up to 29.4 ± 21.9 g m^{-2} d^{-1} in the 24 h LED culture. Negative daytime productivities were significantly associated to a lower number of total photons received from the sun and LEDs combined ($p < 0.05$), as well as lower average temperatures ($p < 0.10$) (Supplementary Fig. S4). The values of areal productivities obtained lie within the interval found for RWPs, i.e. 15–45 g m^{-2} d^{-1} [2,43], with values of 20–25 g m^{-2} d^{-1} being more common in short operations [6].

Global productivities were 9.5 ± 3.0, 12.8 ± 3.2 and 16.5 ± 4.9 g m^{-2} d^{-1} for the control, Night LED and 24 h LED, respectively. The productivity of 24 h LED-lit cultures were almost double the value of the control, and was also higher than previous studies using *N. gaditana* with 14 g m^{-2} d^{-1} and *N. salina* with 13.5 g m^{-2} d^{-1} using similar culture depths of 0.11 and 0.12 m and approximate volumes 800 and 300 L, respectively [44,45]. Previous studies using RWP with higher column depths of 0.25 m with similar areas of 1.2 and 3 m^2 reported areal productivities of 8.3 g m^{-2} d^{-1} for *Nannochloropsis oculata* and 3.3 for *N. salina* [46,47]. Compared to our study, LEDs brought about a significant improvement, particularly considering the lower column depth used in this trial (0.10 m).

3.1.2. Metabolite productivities and contents

Pigment analysis, in terms of chlorophyll and carotenoids, and gross biochemical composition, in terms of lipids, protein, and carbohydrates, were performed on the resulting biomass samples of the small-scale preliminary experiment. Variations in the productivities were compared between the three different conditions (control, night LED, and 24 h LED) according to evening and morning samples of the late exponential growth phase using the averaged samples from the last two days of cultivation of each run (Fig. 5).

Compared to the control culture (evening: 1.79 ± 1.19 mg L^{-1} d^{-1}; morning: 1.37 ± 0.86 mg L^{-1} d^{-1}), a significant increase ($p < 0.05$) in chlorophyll productivities of the cultures grown under the 24 h LED condition (evening: 3.16 ± 0.66 mg L^{-1} d^{-1}; morning: 3.28 ± 1.50 mg L^{-1} d^{-1}) was detected. This is in agreement with previous reports of higher pigment content per cell of *Nannochloropsis gaditana* by the end of the light period [48] when biomass concentrations are also higher, thus contributing to the higher chlorophyll productivities. Even though chlorophyll content was lower in this study (1.84 ± 0.11% f DW) than previous studies using *N. oceanica* with 2.33% of DW [49] and 3.9% of DW [50], carotenoids (0.42 ± 0.02% of DW) were higher than those reported previously [49] (Supplementary Table S2). This could be due to the differences between indoor and outdoor experiments where cells are exposed to much higher irradiances, leading to the activation of photoprotective pathways [50].

At the late exponential phase, the biomass of *N. oceanica* was mainly composed of protein and carbohydrates, with lower lipid contents (see Supplementary Table S2). Control cultures exhibited lipid productivities of 21.8 ± 10.8 and 17.3 ± 10.7 mg L^{-1} d^{-1}, protein productivities of 39.0 ± 11.1 and 36.1 ± 13.8 mg L^{-1} d^{-1}, and carbohydrate productivities of 40.0 ± 13.9 and 33.3 ± 11.7 mg L^{-1} d^{-1}, in evening and morning samples, respectively. Overall, cultures grown under 24 h LEDs presented significantly ($p < 0.05$) higher productivities in terms of protein (evening: 70.3 ± 18.1 mg L^{-1} d^{-1}; morning: 68.8 ± 22.0 mg L^{-1} d^{-1}) and carbohydrates (evening: 69.6 ± 17.2 mg L^{-1} d^{-1}; morning: 64.5 ± 16.0 mg L^{-1} d^{-1}) than those of the control. This can be partially justified by the differences found in DW, as both pigment and macronutrient productivities were lower in the control cultures. The biomass analysis revealed higher chlorophyll, protein, and carbohydrate productivities in the 24 h hour LED-lit cultures, thus contributing to an increased valorization of LED-grown cultures. Biomass composition was similar to a previous study using *N. oceanica* grown outdoors in tubular PBR [3] and the low lipid contents observed suggests that the cells were growing in the absence of nutrient stress [49,51]. Higher differences were expected between productivities of morning and evening samples due to diel regulated metabolisms [33,52]. Nonetheless, lipid productivities were higher using LED-lit cultures – mainly due to the higher biomass productivity of LED-lit cultures – than a previous study cultivating *N. oculata* in 200-L RWP resulting in 25 mg L^{-1} d^{-1} [46]. After pigments, lipids possess the highest market value compared to carbohydrates and lipids [53]. Biomass composition, particularly in terms of high-value metabolites, can valorize the microalgal biomass and render the application of LEDs economically feasible.

Fatty acid profiles were also determined in *N. oceanica* cultures. Saturated fatty acids (SFA) corresponded to myristic (C14:0 < 5.8% of total fatty acids; TFA) and palmitic (C16:0) acids with contents ranging within 20.8–23.0% of TFA; while monounsaturated fatty acids (MUFA), composed of palmitoleic (C16:1) and oleic (C18:1 < 2.5% of TFA) acids, varied within 31.1–34.3% of TFA. PUFA, consisting of linoleic (C18:2 < 4.4% of TFA), arachidonic (C20:4*n*-3) and eicosapentaenoic (EPA;

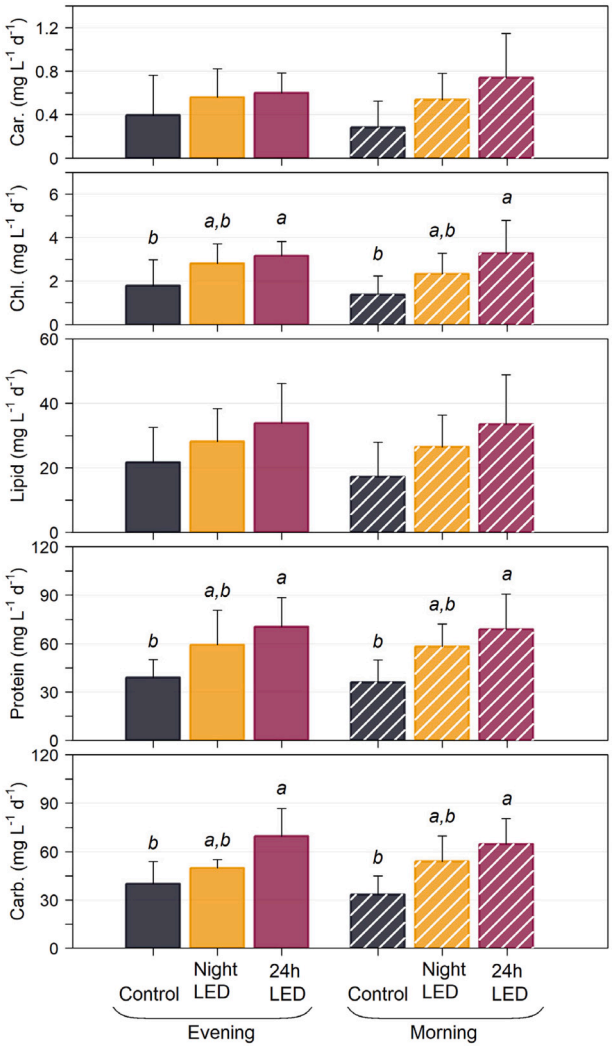

Fig. 5. Volumetric productivities (mg L^{-1} d^{-1}) of pigments in terms of carotenoids (Car.; A) and chlorophyll (Chl; B) and macronutrients, namely lipids (C), protein (D) and carbohydrates (Carb.; E) of *Nannochloropsis oceanica* grown under three different conditions: without LEDs (Control; dark grey), with LEDs turned on during the night (Night LED; yellow) and with LEDs turned on for 24 h (24 h LED; red) in outdoor raceway ponds. Results are expressed as the average of the last two days (late exponential phase) of the three runs, grouped according to evening (solid bars) and morning (striped bars) samples. Different letters represent significant differences ($p < 0.05$) between conditions of the same time sampling group (evening or morning). Absence of letters means no statistical differences were detected between conditions. Error bars represent standard deviations. (For interpretation of the references to colour in this figure legend, the reader is referred to the web version of this article.)

C20:5*n*-6) acids, varied between 43.6 and 47.5% of TFA. The most abundant fatty acids in all cases were palmitoleic and eicosapentaenoic acids. The variation of the main fatty acids (higher than 10% of TFA) in *N. oceanica*, grown under each condition, is shown in Table 1.

The reported fatty acids are consistent with those commonly found in the literature for this genus [3,28,33,54,55]. Furthermore, natural fluctuations of SFA and PUFA, between evening and morning samples, are consistent with the results previously described for *N. oceanica* [33,54], with EPA being significantly ($p < 0.05$) higher in the morning.

Nonetheless, TFA composition was affected by LEDs, resulting in a significant ($p < 0.05$) increase in MUFA, particularly from palmitoleic acid, in both night LED and 24 h LED cultures, in both evening and morning samples. Regardless, PUFA remained the major constituent of TFA, and were primarily composed by the structural EPA. Although lipid

Table 1
Percentage of total fatty acid (% of TFA) of *Nannochloropsis oceanica* grown under three different conditions: without LEDs (control), with LEDs turned on during the night (Night LED), and with LEDs turned on for 24 h (24 h LED) in three outdoor raceway ponds. Results are expressed as mean ± standard deviation of the last two days (late logarithmic phase) of the three runs, grouped according to evening and morning samples. Different letters represent significant differences between conditions of the same time sampling group (evening or morning). Letters were omitted when no significant differences were detected.

	Evening			Morning		
	Control	Night LED	24 h LED	Control	Night LED	24 h LED
C16:0	18.6 ± 2.9	16.9 ± 2.9	16.9 ± 2.4	17.5 ± 2.8	15.9 ± 2.4	15.2 ± 1.0
C16:1	29.6 ± 1.0 (b)	32.5 ± 0.2 (a)	31.8 ± 1.2 (a)	29.0 ± 2.3 (b)	31.7 ± 0.8 (a)	33.0 ± 1.0 (a)
C20:4*n*-6	13.8 ± 2.0	10.1 ± 3.2	11.2 ± 3.9	11.9 ± 4.4	11.6 ± 3.4	8.7 ± 3.0
C20:5*n*-3	26.0 ± 0.7 (b)	28.7 ± 0.7 (a)	26.7 ± 0.2 (b)	30.0 ± 2.5	28.7 ± 1.8	31.4 ± 1.0
SFA	23.0 ± 3.3	22.4 ± 3.7	22.8 ± 3.0	21.4 ± 3.3	21.3 ± 2.8	20.8 ± 1.6
MUFA	32.1 ± 1.2 (b)	34.0 ± 0.1 (a)	33.2 ± 1.1 (a,b)	31.1 ± 2.2 (b)	33.2 ± 0.6 (a,b)	34.3 ± 1.2 (a)
PUFA	44.9 ± 3.3	43.6 ± 3.8	44.0 ± 2.5	47.5 ± 5.0	45.5 ± 2.6	44.9 ± 2.4

productivities were low compared to protein and carbohydrate (Fig. 5), the high EPA content in TFA points to a high valorization of this fraction that can potentially increase the value of the final biomass.

3.1.3. Fluorescence

ETR can function as a proxy for the rate of electrons transported through the photosynthetic chain, providing additional insight into light-limited, saturated, or inhibited intervals for the cultures [56]. Hence, RLCs and photosynthetic efficiency values (α; slopes in dashed lines) were classified according to the growth phase, for both evening and morning samples (Supplementary Fig. S5). All RLCs declined over time, except those of the control culture in the morning during the exponential phase. However, photosynthetic efficiency values decreased with growth, with a more noticeable decrease of the control culture.

The intercept of α with $rETR_{max}$ supports the determination of the minimum saturating irradiance coefficient, E_k. Values above E_k are characterized by a low photosynthetic rate, which competes with energy dissipation [57]. Specific values for E_k are displayed in Table 2.

Results pertaining to E_k were similar for the cultures grown with LEDs where values also decreased with the cultures' growth in both

Table 2
Average of light-saturation (E_k) coefficients determined from rETR versus PAR curves, shown in Supplementary Fig. S5 for *Nannochloropsis oceanica* cultures grown under three different conditions: without LEDs (Control), with LEDs turned on during the night (Night LED), and with LEDs turned on for 24 h (24 h LED) in three 3.0-m^2 raceway ponds outdoors. Results are expressed as mean ± standard deviation of grouped values according to growth phase: lag, logarithmic (log), and late logarithmic (late log) for evening and morning samples. Different letters depicted between brackets represent significant differences ($p < 0.05$) among conditions.

Growth phase	Evening E_k (μmol m^{-2} s^{-1})			Morning E_k (μmol m^{-2} s^{-1})		
	Control	Night LED	24 h LED	Control	Night LED	24 h LED
Lag	321 ± 30	323 ± 26	307 ± 27	258 ± 76	261 ± 49	279 ± 62
Log	348 ± 53	298 ± 46	297 ± 33	333 ± 52 (a)	260 ± 48 (b)	264 ± 47 (b)
Late log	360 ± 30 (a)	261 ± 38 (b)	271 ± 14 (b)	317 ± 61 (a)	244 ± 47 (a,b)	239 ± 41 (b)

evening and morning samples. However, the results from the control increased with growth, showing significantly ($p < 0.05$) higher E_k than LED-lit cultures. Conversely, in morning samples, they peaked during the exponential phase. This suggests that, during dark periods (morning samples), the minimum light requirements were met by using LEDs supplying ca. 318 μmol m^{-2} s^{-1}, which was in fact above the E_k of LED-lit cultures. E_k values are in accordance with a previous study using *Nannochloropsis* cultivated in a FP-PBR (5 cm) and in a high rate algal pond (HRAP; 35 cm) where lower values were found for the more light limited system – HRAP – with light intensities between 264 and 162 μmol m^{-2} s^{-1} [58] The slightly higher values found in our study could be explained by the lower column depth used (10 cm), which favored the light acclimation of the cells. However, it is interesting to note that the LEDs did not produce the same effect. While in the control E_k increased over time (in a culture undergoing higher self-shading due to higher cell concentrations), the LED-lit cultures presented the opposite effect, suggesting that LED-lit cultures were receiving excess light.

3.2. Pilot-scale trials

Considering the small-scale preliminary experiment results, the use of LEDs during the daytime was deemed as not helpful until the culture reached ≈0.5 g DW L^{-1} (column depth of 0.10 m) when dark zones appeared during the day, due to sunlight attenuation in the culture column. Moreover, the LED light intensity tested (ca. 318 μmol m^{-2} s^{-1}) was saturating (E_k: 239–360 μmol m^{-2} s^{-1}). Based on these findings, the experimental setting was scaled up using 24 h LEDs only after the culture surpassed ≈0.5 g DW L^{-1} and tested if a photon-limiting light intensity (below E_k) would still benefit growth while minimizing LED usage and operational costs.

3.2.1. Growth

In this trial, *N. oceanica* cultures started from concentrations of 0.29 ± 0.01 g DW L^{-1} and reached up to 1 g DW L^{-1}, with growth rates strongly affected by available irradiance. Averaged growth curves for both normal and economy modes are shown in Fig. 6A and B, respectively, together with the corresponding averaged specific areal productivities as depicted in Fig. 6C and D.

In normal mode, the control reached an average biomass concentration of 0.95 ± 0.12 g DW L^{-1}, while the LED-lit cultures (72 W m^{-2}) attained 1.1 ± 0.14 g DW L^{-1}. The trial under this mode was cut short to 10 days since the cultures grew faster due to higher temperature and solar irradiance, which were indeed closer to the optimal values for this species (Supplementary Figs. S6 and S7 for normal and economy modes,

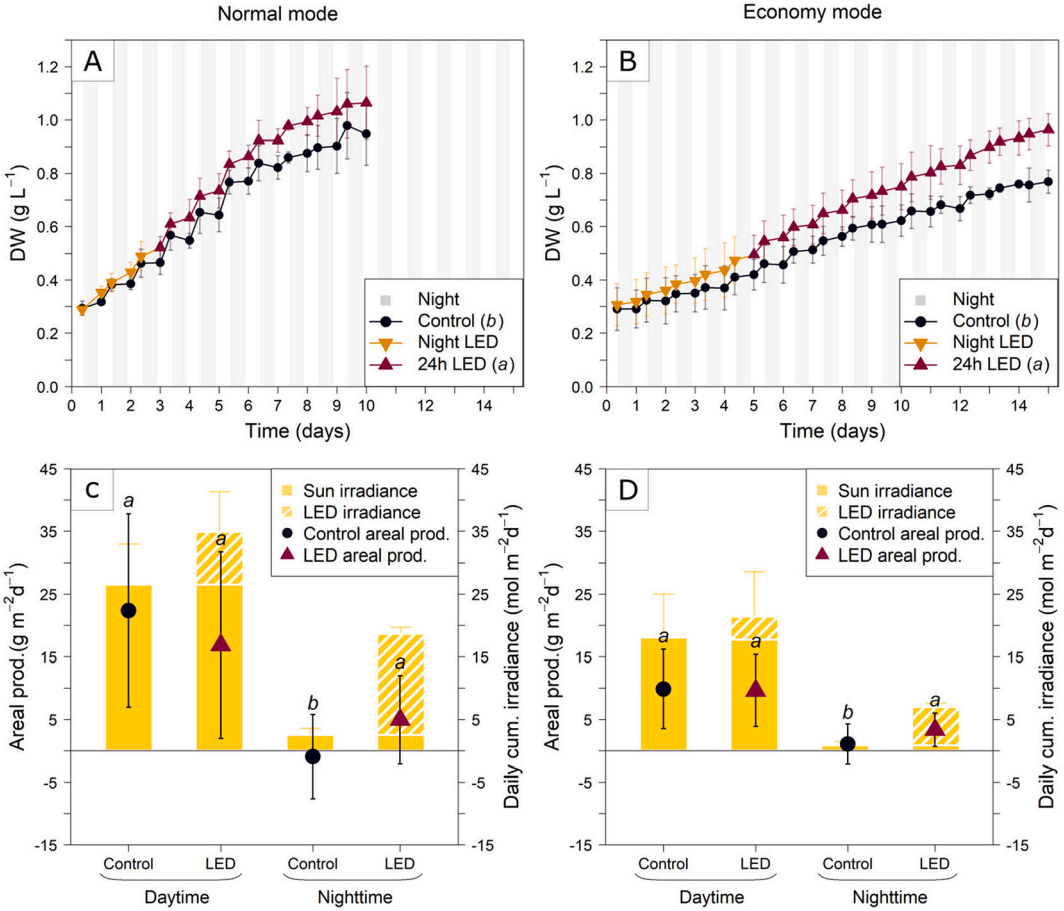

Fig. 6. Averaged growth curves of three independent runs, using *Nannochloropsis oceanica* cultures, in g of dry weight (DW) L^{-1}, for each normal (A) and economy (B) modes of the pilot-scale trial where cultures were grown under two different conditions: without LEDs (control; dark blue circles), and with LEDs (Night LED; yellow inverted triangles and 24 h LED; red triangles) in 28.9-m^2 outdoor raceway ponds. Light grey vertical bars represent the night periods. Conditions that do not share a letter (in brackets in the legend) represent significant differences ($p < 0.05$). In the two lower panels, the average daily specific areal productivities (Areal prod. in g m^{-2} d^{-1}; left Y-axis) is shown, for the control (dark blue circles) and LED-lit (red triangles) cultures during the day and nighttime under normal (C) and economy (D) modes. The bar plot represents the daily averaged photons received by the cultures from day 0 to the end of the experiments (Daily cum. Irradiance in mol m^{-2} d^{-1}; right Y-axis) that originated from the sun (yellow solid bars) and the LEDs (yellow striped bars). Sun irradiance present during nighttime corresponds to the remaining irradiance between evening and morning samples (see Methods section 2.2.2. Pilot-scale trial). Conditions (control versus LED) that do not share a letter within each day and nighttime represent significant differences ($p < 0.05$). Error bars represent standard deviations. (For interpretation of the references to colour in this figure legend, the reader is referred to the web version of this article.)

respectively). After 15 days in the economy mode, the control cultures reached 0.77 ± 0.04 g DW L^{-1} while the LED-lit culture (29 W m^{-2}) reached 0.96 ± 0.06 g DW L^{-1}. In both trials, cultures lit with LEDs grew significantly faster ($p < 0.05$) than their respective controls, with a higher difference to the control in the economy mode trial.

The lower sun irradiance and temperature observed during economy mode runs made the additional LED lighting more effective. This effect can be seen in Fig. 6C and D, which show the average daily specific areal productivities of the cultures grown with LEDs during the day and nighttime, for each cultivation mode, together with the total daily photons received per day by the cultures from the sun and the LEDs.

Areal daily productivities for control cultures, under normal mode, reached 22.4 ± 15.4 and −0.91 ± 6.70 of g m^{-2} d^{-1} in the day and nighttime, respectively, while receiving 26.5 ± 6.4 mol of photons m^{-2} d^{-1}. For this trial, areal daily productivities of the LED-lit cultures were not significantly different (16.9 ± 14.9 g m^{-2} d^{-1}) than that of the control during daytime. However, they were able to prevent biomass loss during the nighttime, with productivities of 4.97 ± 7.06 g m^{-2} d^{-1}, while receiving an additional 8.4 (after LEDs were left on for 24 h) and 16.1 mol of photons m^{-2} d^{-1} from the LEDs during the day and nighttime, respectively. This is not surprising, in view of the positive relationship between growth and respiration arising from the cost of biomass synthesis [59], and further explains the lower daytime productivities in LED-lit cultures.

In the economy-mode experiment(Fig. 6D), average areal daily productivities in the control cultures reached 9.88 ± 6.33 and 1.08 ± 3.22 of g m^{-2} d^{-1} in the day and nighttime, respectively, while receiving 18.1 ± 6.9 mol of photons m^{-2} d^{-1} from the sun. Control and LED-lit cultures displayed similar productivities during the daytime (9.64 ± 5.72 g m^{-2} d^{-1}). However, the latter showed higher values during nighttime (3.37 ± 2.66 g m^{-2} d^{-1}) compared to those of the control, while receiving 3.7 and 6.2 mol of additional photons m^{-2} d^{-1} from the LEDs during the day and nighttime, respectively, upon leaving these lights on for 24 h. For both modes, significant differences ($p < 0.05$) were found between LED lighting conditions and controls during nighttime only. Areal productivities found in the pilot-scale trial are consistent with those previously reported in these RWP with a maximum of 18.1 g m^{-2} d^{-1} (considering a similar operation to the current trial) using *N. oceanica* [28]. Nonetheless, cultures in large commercial RWP rarely exceed 12–13 g m^{-2} d^{-1} [6]. Global productivities in the pilot trials were lower compared to the preliminary experiment with 8.79 ± 1.87 and 10.44 ± 2.09 g m^{-2} d^{-1} for the control and LED lit culture in normal mode, and 4.24 ± 0.44 and 5.82 ± 0.38 g m^{-2} d^{-1} for the control and LED lit culture in economy mode, respectively. The economy mode values are lower than those reported in RWP under similar conditions with 9.7 and 7.7 g m^{-2} d^{-1} using *Nannochloropsis* sp. and *N. oceanica* in 4.73 and 2.89 m^3 with 0.2 and 0.1 m of column depth [28,60]. However, the LED-lit culture in normal mode was able to surpass both values.

It is interesting to note that the control culture from the normal mode experiment received almost the same daily photons (29.1 mol of photons m^{-2} d^{-1}) as the LED-lit culture in the economy mode experiment (28.4 mol of photons m^{-2} d^{-1}). However, areal productivities between the two conditions varied considerably, owing to the increase in average temperatures and the faster growth during normal mode, which increased the extension of dark zones in RWPs. LED irradiance (72 W m^{-2}) was thus rendered less efficient due to higher light attenuation in the culture column. In this sense, the application of LEDs in microalgae cultivation seems to be more useful under lower sunlight irradiances, such as in winter or at low irradiance locations. This agrees with the different specific areal productivities found in the small-scale preliminary experiment, for which higher differences from control values were found for microalgae being grown under lower sun irradiances during the first run.

3.2.2. LED operation costs

In industrial applications, increased biomass productivity can be meaningless if additional costs are not accounted for. Table 3 presents the pilot-scale trial data considering the extra investment and biomass return, compared to the corresponding controls. Table 3 shows the depreciated initial additional investment in LED strips, and the necessary power supplies as well as the operational costs in terms of the additional electricity spent during an operational period of 330 days per year.

According to the pilot-scale trial results, yearly operation would result in 21 and 19.8 kg of additional biomass compared to that of the control, if the normal or economic modes were chosen, respectively. Even though LED modes (normal and economy) do not differ substantially in terms of additional biomass produced, their production costs do. The resulting 21 kg of extra biomass using the normal mode led to an additional expense of 208 € kg^{-1}. In contrast, this value drops to less than half, 91 € kg^{-1}, for almost the same extra biomass (20 kg) from cultures grown under economy mode. Considering an average productivity of 2.7 kg m^{-2} $year^{-1}$ for the south of Spain [53], the extra biomass produced owing to the LED lighting (0.70 ± 0.02 kg m^{-2} $year^{-1}$) accounts for an increase by 25% of the yearly produced biomass.

For a 100-ha facility with productivities between 21 and 27 ton ha^{-1} $year^{-1}$, production costs have been previously reported to lie around 4.95 and 5.20 € kg^{-1} [53,61], respectively. However, increasing the production scale can also lead to lower production costs [2,4]. In addition, a more concentrated culture reduces the culture volume to be processed, decreasing the biomass separation costs in the downstream process, since harvesting from RWPs can contribute with ca. 23% of the overall cultivation costs [53].

To compare overall photosynthetic efficiency (PE) conversion of luminous energy from the sun and LEDs to biomass were determined according to the biomass energy content of 22.2 MJ Kg^{-1} [62]. This resulted in values of 1.49 ± 0.34 and 1.08 ± 0.16% for the control of LED-lit cultures under normal cultivation and 1.09 ± 0.13 and 1.11 ± 0.17% for the control and LED-lit cultures under economy cultivation. PE increased greatly in the normal mode, when sun irradiance was stronger, thus characterizing this light-limited cultivation system. On the other hand, PE of LED-lit cultures remained constant for the cultivation of both modes enhancing the possible need of LED application only in light limited situations together with high-value applications of the biomass. As the LED efficiency in RWPs is dependent on weather conditions, particularly sunlight (since LEDs are more efficient at lower sun irradiances), as well as biomass density, continuous fine-tuning of the LED operation time can lead to more promising results in terms of value of the additional biomass produced. Even so, the feasibility of application should only be considered for high-value products, when sunlight is limiting at high latitude locations and/or under wintery weather conditions.

Table 3
Parameters of the LEDs used for the LED conditions in the pilot-scale trial, under normal and economy modes. An average usable life of 30.000 h for the LEDs and the power supply was used to determine the depreciation value for an yearly 330-day operation. Means of the resulting biomass in each mode were used as a proxy for the biomass produced without taking into account seasonal variations.

Parameters	Pilot-scale trial		Units
	Normal	Economy	
LED strips	794.37	317.75	€ $year^{-1}$
Power supply	410.65	186.66	€ $year^{-1}$
$CAPEX_{LED}$	1205.02	504.41	€ $year^{-1}$
Electricity	3152.33	1302.54	€ $year^{-1}$
$CAPEX_{LED}$ + $OPEX_{LED}$	4357.34	1806.94	€ $year^{-1}$
Extra biomass produced[a]	21.0	19.8	kg $year^{-1}$
Cost of extra biomass produced[a]	207.58	91.12	€ kg^{-1}

[a] Extra biomass produced compared to the respective control.

4. Conclusions

The application of LEDs in outdoor RWPs increased biomass growth mainly by increasing nighttime productivities. Consequently, a positive outcome was attained in terms of nutrient productivity, particularly protein and carbohydrates. The use of LEDs proved more efficient under low irradiances in both small-scale and pilot-scale cultures. The E_k coefficient was helpful to determine a more economical LED setup within the light-limited region for the pilot-scale trials. The economy mode also proved more efficient, yielding almost the same extra biomass under normal mode, at less than half the cost. The incorporation of solar panels to generate electricity could, in the long run, appear as beneficial in terms of sustaining LED operation and diminishing OPEX [63]. In any case, the incorporation of LEDs should be mainly considered for high-value products.

Statement of informed consent, human/animal rights

No conflicts, informed consent, human or animal rights applicable.

CRediT authorship contribution statement

Carneiro, M.: Conceptualization, Methodology, Investigation, Data analysis, Visualization, Writing - Original draft, review, and editing.

Maia, I.B., Cunha, P., Guerra, I.: Investigation, Methodology, Data analysis, Writing – review.

Magina, T., Santos, T.: Investigation, Data analysis, Writing – review.

Schulze, P.S.C.: Conceptualization, Data analysis, Writing – review & editing.

Pereira, H.: Conceptualization, Methodology, Resources, Writing – review.

Malcata, F.X.: Resources, Writing – review, Supervision.

Navalho, J., Silva, J.: Conceptualization, Resources, Writing – review, Funding acquisition.

A. Otero: Data analysis, Writing – review & editing, Supervision.

J. Varela: Conceptualization, Resources, Writing – review, Supervision, Project administration, Funding acquisition.

Declaration of competing interest

The authors declare that they have no known competing financial interests or personal relationships that could have appeared to influence the work reported in this paper.

Acknowledgments

The authors kindly thank Dr. Barreto for consultation assistance, Dr. Gomes and Dr. Correia for experimental support, and Dr. Serôdio for providing a fluorescence analysis model.

The authors are grateful to the companies Necton S.A. and Allmicroalgae S.A., for providing the necessary access and supplies to perform the experiments, Exaktor S.A. for support on LEDs, and the Portuguese Institute for Sea and Atmosphere, I. P. (IPMA, IP) for providing weather data.

This work was jointly supported by the doctoral research grant SFRH/BD/129952/2017 from the Foundation for Science and Technology (FCT); as well as ALGAVALOR - MicroALGAe: integrated production e VALORization of biomass and its diverse applications, POCI-01-0247-FEDER-035234, LISBOA-01-0247-FEDER-035234, ALG-01-0247-FEDER-035234 and Portuguese national funds from FCT through project UIDB/04326/2020; base funding for Laboratory for Process Engineering, Environment, Biotechnology, and Energy – LEPABE – funded by national funds through the FCT/MCTES (PIDDAC) [UIDB/00511/2020]; operational programs CRESC Algarve 2020 and COMPETE 2020 through project EMBRC.PT ALG-01-0145-FEDER-022121; and project DINOSSAUR—PTDC/BBB-EBB/ 1374/2014-POCI-01-0145-FEDER-016640, funded by FEDER funds through COMPETE2020 – Programa Operacional Competitividade e Internacionalização (POCI), and by national funds through FCT.

Appendix A. Supplementary data

Supplementary data to this article can be found online at https://doi.org/10.1016/j.algal.2022.102685.

References

[1] J.W. Richardson, M.D. Johnson, J.L. Outlaw, Economic comparison of open pond raceways to photo bio-reactors for profitable production of algae for transportation fuels in the southwest, Algal Res. 1 (2012).
[2] F.G. Acién, J.M. Fernández, J.J. Magán, E. Molina, Production cost of a real microalgae production plant and strategies to reduce it, Biotechnol. Adv. 30 (2012) 1344–1353, https://doi.org/10.1016/j.biotechadv.2012.02.005.
[3] I. Guerra, H. Pereira, M. Costa, J.T. Silva, T. Santos, J. Varela, M. Mateus, J. Silva, Operation regimes: a comparison based on nannochloropsis oceanica biomass and lipid productivity, Energies. 14 (2021) 1542, https://doi.org/10.3390/en14061542.
[4] B. Llamas, M.C. Suárez-Rodríguez, C.V. González-López, P. Mora, F.G. Acién, Techno-economic analysis of microalgae related processes for CO2 bio-fixation, Algal Res. 57 (2021), 102339, https://doi.org/10.1016/j.algal.2021.102339.
[5] R. Davis, A. Aden, P.T. Pienkos, Techno-economic analysis of autotrophic microalgae for fuel production, Appl. Energy 88 (2011) 3524–3531, https://doi.org/10.1016/j.apenergy.2011.04.018.
[6] M.R. Tredici, Mass production of microalgae: photobioreactors, in: Handb. Microalgal Cult, Blackwell Publishing Ltd, Oxford, UK, 2004, pp. 178–214, https://doi.org/10.1002/9780470995280.ch9.
[7] G. Khawam, P. Waller, S. Gao, S. Edmundson, M. Huesemann, S. Attalah, K. L. Ogden, Simulation of shading and algal growth in experimental raceways, Algal Res. 41 (2019), 101575, https://doi.org/10.1016/j.algal.2019.101575.
[8] M. Huesemann, T. Dale, A. Chavis, B. Crowe, S. Twary, A. Barry, D. Valentine, R. Yoshida, M. Wigmosta, V. Cullinan, Simulation of outdoor pond cultures using indoor LED-lighted and temperature-controlled raceway ponds and phenometrics photobioreactors, Algal Res. 21 (2017) 178–190, https://doi.org/10.1016/j.algal.2016.11.016.
[9] Y. Chisti, Large-scale production of algal biomass: raceway ponds, in: Algae Biotechnol. Green Energy Technol, 2016, pp. 21–40, https://doi.org/10.1007/978-3-319-12334-9_2.
[10] A. Vonshak, S. Laorawat, B. Bunnag, M. Tanticharoen, The effect of light availability on the photosynthetic activity and productivity of outdoor cultures of Arthrospira platensis (Spirulina), J. Appl. Phycol. 26 (2014) 1309–1315, https://doi.org/10.1007/s10811-013-0133-1.
[11] J.U. Grobbelaar, C.J. Soeder, Respiration losses in planktonic green algae cultivated in raceway ponds, J. Plankton Res. 7 (1985) 497–506, https://doi.org/10.1093/plankt/7.4.497.
[12] A. Sánchez Zurano, J.A. Garrido Cárdenas, C. Gómez Serrano, M. Morales Amaral, F.G. Acién-Fernández, J.M. Fernández Sevilla, E. Molina Grima, Year-long assessment of a pilot-scale thin-layer reactor for microalgae wastewater treatment. Variation in the microalgae-bacteria consortium and the impact of environmental conditions, Algal Res. 50 (2020), 101983, https://doi.org/10.1016/j.algal.2020.101983.
[13] H. Pereira, J. Páramo, J. Silva, A. Marques, A. Barros, D. Maurício, T. Santos, P. Schulze, R. Barros, L. Gouveia, L. Barreira, J. Varela, Scale-up and large-scale production of Tetraselmis sp. CTP4 (Chlorophyta) for CO2 mitigation: from an agar plate to 100–m3 industrial photobioreactors, Sci. Rep. 8 (2018), https://doi.org/10.1038/s41598-018-23340-3.
[14] G. Torzillo, G.Chini Zittelli, Tubular photobioreactors, in: Algal Biorefineries, Springer International Publishing, Cham, 2015, pp. 187–212, https://doi.org/10.1007/978-3-319-20200-6_5.
[15] M.R. Tredici, L. Rodolfi, N. Biondi, N. Bassi, G. Sampietro, Techno-economic analysis of microalgal biomass production in a 1-ha Green Wall panel (GWP®) plant, Algal Res. 19 (2016) 253–263, https://doi.org/10.1016/j.algal.2016.09.005.
[16] A. San Pedro, C.V. González-López, F.G. Acién, E. Molina-Grima, Outdoor pilot production of Nannochloropsis gaditana: influence of culture parameters and lipid production rates in flat-panel photobioreactors, Algal Res. 18 (2016) 156–165, https://doi.org/10.1016/j.algal.2016.06.011.
[17] A. Morillas-España, T. Lafarga, C. Gómez-Serrano, F.G. Acién-Fernández, C. V. González-López, Year-long production of Scenedesmus almeriensis in pilot-scale raceway and thin-layer cascade photobioreactors, Algal Res. 51 (2020), 102069, https://doi.org/10.1016/j.algal.2020.102069.
[18] S. Pereira, A. Otero, Effect of light quality on carotenogenic and non-carotenogenic species of the genus dunaliella under nitrogen deficiency, Algal Res. 44 (2019), 101725, https://doi.org/10.1016/j.algal.2019.101725.
[19] E.G. Nwoba, D.A. Parlevliet, D.W. Laird, K. Alameh, N.R. Moheimani, Light management technologies for increasing algal photobioreactor efficiency, Algal Res. 39 (2019), 101433, https://doi.org/10.1016/j.algal.2019.101433.

[20] D. Demory, C. Combe, P. Hartmann, A. Talec, E. Pruvost, R. Hamouda, F. Souillé, P. O. Lamare, M.O. Bristeau, J. Sainte-Marie, S. Rabouille, F. Mairet, A. Sciandra, O. Bernard, How do microalgae perceive light in a high-rate pond? Towards more realistic lagrangian experiments, R. Soc. Open Sci. 5 (2018), https://doi.org/10.1098/rsos.180523.

[21] P.S.C. Schulze, H.G.C. Pereira, T.F.C. Santos, L. Schueler, R. Guerra, L.A. Barreira, J.A. Perales, J.C.S. Varela, Effect of light quality supplied by light emitting diodes (LEDs) on growth and biochemical profiles of Nannochloropsis oculata and Tetraselmis chuii, Algal Res. 16 (2016) 387–398, https://doi.org/10.1016/j.algal.2016.03.034.

[22] P.S.C. Schulze, L.A. Barreira, H.G.C. Pereira, J.A. Perales, J.C.S. Varela, Light emitting diodes (LEDs) applied to microalgal production, Trends Biotechnol. 32 (2014) 422–430, https://doi.org/10.1016/j.tibtech.2014.06.001.

[23] J. Masojídek, K. Ranglová, G.E. Lakatos, A.M. Silva Benavides, G. Torzillo, Variables governing photosynthesis and growth in microalgae mass cultures, Processes. 9 (2021) 820, https://doi.org/10.3390/pr9050820.

[24] E.M. Radmann, C.O. Reinehr, J.A.V. Costa, Optimization of the repeated batch cultivation of microalga Spirulina platensis in open raceway ponds, Aquaculture 265 (2007) 118–126, https://doi.org/10.1016/j.aquaculture.2007.02.001.

[25] R.R.L. Guillard, J.H. Ryther, Studies of marine planktonic diatoms: I. Cyclotella nana Hustedt, and Detonula confervacea (Cleve) Gran, Can. J. Microbiol. 8 (1962) 229–239, https://doi.org/10.1139/m62-029.

[26] M. Olofsson, T. Lamela, E. Nilsson, J.P. Bergé, V. del Pino, P. Uronen, C. Legrand, Seasonal variation of lipids and fatty acids of the microalgae Nannochloropsis oculata grown in outdoor large-scale photobioreactors, Energies 5 (2012) 1577–1592, https://doi.org/10.3390/en5051577.

[27] R.B. Baird, A.D. Eaton, E.W. Rice (Eds.), Standard Methods for the Examination of Water and Wastewater, 23rd ed., American Public Health Association, American Water Works Association, Water Environment Federation, 2017.

[28] P. Cunha, H. Pereira, M. Costa, J. Pereira, J.T. Silva, N. Fernandes, J. Varela, J. Silva, M. Simões, Nannochloropsis oceanica cultivation in pilot-scale raceway ponds—from design to cultivation, Appl. Sci. 10 (2020) 1725, https://doi.org/10.3390/app10051725.

[29] H. Morkoç, Light-emitting diodes and lighting, in: Handb. Nitride Semicond. Devices. Vol. 3 GaN-Based Opt. Electron. Devices, WILEY-VCH Verlag GmbH & Co. KGaA, Weinheim, 2009, p. 902.

[30] C.J. Zhu, Y.K. Lee, Determination of biomass dry weight of marine microalgae, J. Appl. Phycol. 9 (1997) 189–194, https://doi.org/10.1023/A:1007914806640.

[31] B. Genty, J.M. Briantais, N.R. Baker, The relationship between the quantum yield of photosynthetic electron transport and quenching of chlorophyll fluorescence, Biochim. Biophys. Acta Gen. Subj. 990 (1989) 87–92, https://doi.org/10.1016/S0304-4165(89)80016-9.

[32] P.H.C. Eilers, J.C.H. Peeters, A model for the relationship between light intensity and the rate of photosynthesis in phytoplankton, Ecol. Model. 42 (1988) 199–215, https://doi.org/10.1016/0304-3800(88)90057-9.

[33] M. Carneiro, B. Cicchi, I.B. Maia, H. Pereira, G.C. Zittelli, J. Varela, F.X. Malcata, G. Torzillo, Effect of temperature on growth, photosynthesis and biochemical composition of nannochloropsis oceanica, grown outdoors in tubular photobioreactors, Algal Res. 49 (2020), 101923, https://doi.org/10.1016/j.algal.2020.101923.

[34] SCOR-UNESCO, Determination of photosynthetic pigments in seawater, in: Monogr. Oceanogr. Methodol 1, UNESCO, Paris, 1966.

[35] E.M.J. Jaspars, Pigmentation of tobacco crown-gall tissues cultured in vitro in dependence of the composition of the medium, Physiol. Plant. 18 (1965) 933–940, https://doi.org/10.1111/j.1399-3054.1965.tb06990.x.

[36] E.G.G. Bligh, W.J.J. Dyer, A rapid method of total lipid extraction and purification, Can. J. Biochem. Physiol. 37 (1959) 911–917, https://doi.org/10.1139/o59-099.

[37] H. Pereira, L. Barreira, A. Mozes, C. Florindo, C. Polo, C.V. Duarte, L. Custódio, J. Varela, Microplate-based high throughput screening procedure for the isolation of lipid-rich marine microalgae, Biotechnol. Biofuels. 4 (2011) 61, https://doi.org/10.1186/1754-6834-4-61.

[38] S.O. Lourenço, E. Barbarino, P.L. Lavín, U.M.L. Marquez, E. Aidar, Distribution of intracellular nitrogen in marine microalgae: calculation of new nitrogen-to-protein conversion factors, Eur. J. Phycol. 39 (2004) 17–32, https://doi.org/10.1080/0967026032000157156.

[40] J. Folch, M. Lee, G.H.Sloane Stanley, A simple method for the isolation and purification of total lipides from animal tissues, J. Biol. Chem. 226 (1957).

[41] G. Lepage, C.C. Roy, Improved recovery of fatty acid through direct transesterification without prior extraction or purification, J. Lipid Res. 25 (1984) 1391–1396, https://doi.org/10.1016/S0022-2275(20)34457-6.

[42] J.U. Grobbelaar, Mass production of microalgae at optimal photosynthetic rates, in: Z. Dubinsky (Ed.), Photosynthesis, IntechOpen, 2013, pp. 357–371, https://doi.org/10.5772/55193.

[43] L. Brennan, P. Owende, Biofuels from microalgae—a review of technologies for production, processing, and extractions of biofuels and co-products, Renew. Sust. Energ. Rev. 14 (2010) 557–577, https://doi.org/10.1016/j.rser.2009.10.009.

[44] C. Ledda, G.I. Romero Villegas, F. Adani, F.G. Acién Fernández, E. Molina Grima, Utilization of centrate from wastewater treatment for the outdoor production of Nannochloropsis gaditana biomass at pilot-scale, Algal Res. 12 (2015) 17–25, https://doi.org/10.1016/j.algal.2015.08.002.

[45] S. Boussiba, A. Vonshak, Z. Cohen, Y. Avissar, A. Richmond, Lipid and biomass production by the halotolerant microalga nannochloropsis Salina, Biomass 12 (1987) 37–47, https://doi.org/10.1016/0144-4565(87)90006-0.

[46] A. Millán-Oropeza, L. Fernández-Linares, Biomass and lipid production from nannochloropsis oculata growth in raceway ponds operated in sequential batch mode under greenhouse conditions, Environ. Sci. Pollut. Res. 24 (2017) 25618–25626, https://doi.org/10.1007/s11356-016-7013-6.

[47] B. Crowe, S. Attalah, S. Agrawal, P. Waller, R. Ryan, J. Van Wagenen, A. Chavis, J. Kyndt, M. Kacira, K.L. Ogden, M. Huesemann, A comparison of nannochloropsis Salina growth performance in two outdoor pond designs: conventional raceways versus the ARID pond with superior temperature management, Int. J. Chem. Eng. 2012 (2012) 1–9, https://doi.org/10.1155/2012/920608.

[48] J. Fábregas, A. Maseda, A. Domínguez, M. Ferreira, A. Otero, Changes in the cell composition of the marine microalga, Nannochloropsis gaditana, during a light: dark cycle, Biotechnol. Lett. 24 (2002), https://doi.org/10.1023/A:1020661719272.

[49] M. Carneiro, G. Chini Zittelli, B. Cicchi, E. Touloupakis, C. Faraloni, I.B. Maia, H. Pereira, T. Santos, F.X. Malcata, A. Otero, J. Varela, G. Torzillo, In situ monitoring of chlorophyll a fluorescence in nannochloropsis oceanica cultures to assess photochemical changes and the onset of lipid accumulation during nitrogen deprivation, Biotechnol. Bioeng. 118 (2021) 4375–4388, https://doi.org/10.1002/bit.27906.

[50] B. Wang, J. Jia, Photoprotection mechanisms of nannochloropsis oceanica in response to light stress, Algal Res. 46 (2020), 101784, https://doi.org/10.1016/j.algal.2019.101784.

[51] A. Molino, A. Iovine, P. Casella, S. Mehariya, S. Chianese, A. Cerbone, J. Rimauro, D. Musmarra, Microalgae characterization for consolidated and new application in human food, animal feed and nutraceuticals, Int. J. Environ. Res. Public Heal. 15 (2018), https://doi.org/10.3390/ijerph15112436.

[52] A. Sukenik, Y. Carmeli, Lipid synthesis and fatty acid composition in Nannochloropsis sp. (Eustigmatophyceae) grown in a light-dark cycle, J. Phycol. 26 (1990) 463–469, https://doi.org/10.1111/j.0022-3646.1990.00463.x.

[53] J. Ruiz, G. Olivieri, J. De Vree, R. Bosma, P. Willems, J.H. Reith, M.H.M.M. Eppink, D.M.M.M. Kleinegris, R.H. Wijffels, M.J. Barbosa, Towards industrial products from microalgae, Energy Environ. Sci. 9 (2016) 3036–3043, https://doi.org/10.1039/C6EE01493C.

[54] A. Sukenik, Y. Carmeli, Regulation of fatty acid composition by irradiance level in the eustigmatophyte Nannochloropsis sp, J. Phycol. 25 (1989).

[55] J. Fábregas, A. Maseda, A. Domínguez, A. Otero, The cell composition of Nannochloropsis sp. changes under different irradiances in semicontinuous culture, World J. Microbiol. Biotechnol. 20 (2004) 31–35, https://doi.org/10.1023/B:WIBI.0000013288.67536.ed.

[56] S. Beer, B. Vilenkin, A. Weil, M. Veste, L. Susel, A. Eshel, Measuring photosynthetic rates in seagrasses by pulse amplitude modulated (PAM) fluorometry, Mar. Ecol. Prog. Ser. 174 (1998) 293–300, https://doi.org/10.3354/meps174293.

[57] J.R.F. Malapascua, C.G. Jerez, M. Sergejevová, F.L. Figueroa, J. Masojídek, Photosynthesis monitoring to optimize growth of microalgal mass cultures: application of chlorophyll fluorescence techniques, Aquat. Biol. 22 (2014) 123–140, https://doi.org/10.3354/ab00597.

[58] J.C. Kromkamp, J. Beardall, A. Sukenik, J. Kopecky, J. Masojídek, S. van Bergeijk, S. Gabai, E. Shaham, A. Yamshon, Short-term variations in photosynthetic parameters of nannochloropsis cultures grown in two types of outdoor mass cultivation systems, Aquat. Microb. Ecol. 56 (2009) 309–322, https://doi.org/10.3354/ame01318.

[59] R. Geider, J. Geider, R. Osborne, B.a. Osborne, Respiration and microalgal growth: a review of the quantitative relationship between dark respiration and growth, New Phytol. 112 (1989) 327–341, https://doi.org/10.1111/j.1469-8137.1989.tb00321.x.

[60] J.H. de Vree, R. Bosma, M. Janssen, M.J. Barbosa, R.H. Wijffels, Comparison of four outdoor pilot-scale photobioreactors, Biotechnol. Biofuels. 8 (2015) 215, https://doi.org/10.1186/s13068-015-0400-2.

[61] N.-H. Norsker, M.J. Barbosa, M.H. Vermuë, R.H. Wijffels, Microalgal production — a close look at the economics, Biotechnol. Adv. 29 (2011) 24–27, https://doi.org/10.1016/j.biotechadv.2010.08.005.

[62] M.R. Tredici, N. Bassi, M. Prussi, N. Biondi, L. Rodolfi, G.C. Zittelli, G. Sampietro, Energy balance of algal biomass production in a 1-ha "'green wall panel"' plant : how to produce algal biomass in a closed reactor achieving a high net energy ratio q, Appl. Energy 154 (2015) 1103–1111, https://doi.org/10.1016/j.apenergy.2015.01.086.

[63] M. Morales, A. Hélias, O. Bernard, Optimal integration of microalgae production with photovoltaic panels: environmental impacts and energy balance, Biotechnol. Biofuels. 12 (2019) 239, https://doi.org/10.1186/s13068-019-1579-4.